Investigations into Bluetooth Low Energy Localization Precision Limits

Joerg Schmalenstroeer, Reinhold Haeb-Umbach
Department of Communications Engineering, University of Paderborn, Germany
{schmalen,haeb}@nt.uni-paderborn.de

***Abstract*—In this paper we study the influence of directional radio patterns of Bluetooth low energy (BLE) beacons on smartphone localization accuracy and beacon network planning. A two-dimensional model of the power emission characteristic is derived from measurements of the radiation pattern of BLE beacons carried out in an RF chamber. The Cramer-Rao lower bound (CRLB) for position estimation is then derived for this directional power emission model. With this lower bound on the RMS positioning error the coverage of different beacon network configurations can be evaluated. For near-optimal network planing an evolutionary optimization algorithm for finding the best beacon placement is presented.**

Index Terms: BLE, localization precision, CRLB, evolutionary algorithm

I. Introduction

Location-based services show promise in a variety of application fields. Among them is the scenario of the so-called industry 4.0, where in production facilities the location of tools, workers and goods has to be tracked [1]. Another example is the support of customers during their shopping sprees [2]: Guidance to the requested product, promotion of special offers, or information on ingredients are only a small selection of conceivable applications.

All these services hinge on the availability of precise location information. The task of position estimation can be solved in various ways. Known approaches use visual (barcode, object identification) or acoustic (ultrasound) information, magnetic fields [3], data encoded in light (ceiling lights), radio signals (WLAN, RFID, NFC, BLE) [4], dead reckoning [5] (inertial measurement units), or combinations of the aforementioned modalities [6], [7], [8].

Bluetooth low energy (BLE) based positioning has recently received remarkable attention due to its low installation costs, broad support by mobile end devices (smartphones) and low energy consumption, both on the beacon and on the mobile device side [9]. However, localization based only on BLE usually suffers from low accuracy [10].

In this paper we study the influence of directional radio patterns of BLE beacons on localization precision. Preliminary work has been published by Patwari et al. in [11], where the Cramér-Rao lower bound (CRLB) for omnidirectional characteristics was discussed. Hossain et al. derived the CRLB for a signal strength difference based localization system [12], and the authors of [13] investigated the fundamental performance limitations of a linear fusion approach where multiple measurements from different information sources were combined.

BLE localization is closely coupled with the task of network planing, i.e., deciding where to place the beacons to achieve a minimal localization error. In [14] an overview about common network planing strategies for WiFi systems is presented. Optimal strategies, however, have a computational issue. They tend to be NP-hard because the computational effort grows rapidly with the number of transmitters and the size of space. Introducing a new variable, i.e., the orientation of the beacons, will increase the computational demands even further.

The paper is organized as follows. In Sec. II a 2D-model for the power radiation of the beacons is given, which is based on laboratory measurements. The CRLB on the positioning error is derived in Sec. III using this directional radiation model. Subsequently, the influence of the direction dependency on the RMS error is discussed in the experimental Sec. IV, where the performance of a Maximum Likelihood (ML) estimator is compared with the CRLB. In Sec. V an evolutionary algorithm for near-optimal beacon network planning is presented, and we end up with some conclusions in Sec. VI.

II. RSSI Model

Each beacon emits periodically an advertisement package with a predefined signal strength. Devices receiving these advertisement packages measure the signal strength in terms of the "Received Signal Strength Indicator" (RSSI). The received signal power can be modeled in the logarithmic domain by the following log-normal fading model [8], [12]

$$P = P_0 - 10\eta \ln(d/d_0) + n = \overline{P} + n. \tag{1}$$

Here, P_0 is the RSSI level at reference distance d_0, measured in dB, η is a room specific constant which controls how fast the power decays with the distance from the transmitter, d is the distance between the beacon and the position of the sensing device, and $\overline{P}$ denotes the mean RSSI value at distance d. Further, n is a zero-mean normally distributed random variable, which we call *measurement noise* in the following. From experimental data the values of P_0 and η can be estimated via a least-squares fitting of equation (1) to measurements.

A. Laboratory experiments

Experimental results show that in realistic scenarios the model of equation (1) is not fulfilled. Especially the assumption of a constant reference power P_0 is usually violated by

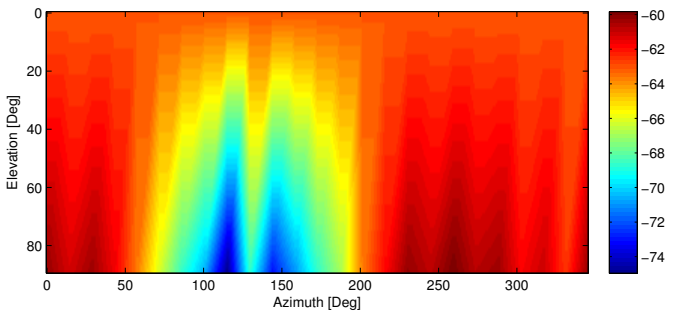

Fig. 1. Measured RSSI values in dB at 1 m distance in antenna lab for different azimuth and elevation angles.

a factor of up to ± 10 dB and thus should be replaced by an angular dependent reference power $P_0(\alpha)$.

We measured the average emitted power of a beacon as a function of the azimuth and the elevation angle in our antenna laboratory using an Android smartphone. The results are depicted in Fig. 1. While these particular results certainly depend on the beacon and smartphone used, and will be different if other devices are employed, it can be observed in general that the radiation pattern of BLE beacons is not omnidirecional. This fact will have a significant impact on the localization accuracy, as we will show.

To simplify our model we reduce the 3D-measurements to a 2D-problem in the following, by selecting the data at 90-degree elevation. This equals a setup where the beacons and the smartphone are placed in the same horizontal plane. However, the derivation of the CRLB in section III should in principle be possible also for 3D-models.

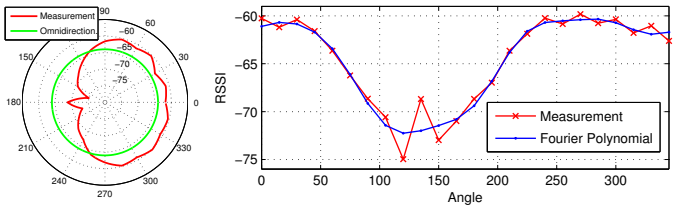

(a) Measurements (b) Fourier polynomial

Fig. 2. Comparison between omnidirectional radiation characteristic ((a) green line), and laboratory measurements ((a) and (b), red curve); approximation of measured radiation pattern by Fourier polynomial of order $m = 6$ ((b) blue curve).

B. Angular dependent RSSI model

The Fig. 2(a)) shows a polar plot of the beacon radiation pattern and compares it with an omnidirectional pattern. The pattern $P(\alpha)$ is measured at M discrete angles $\boldsymbol{\alpha} = [\alpha_1, \ldots, \alpha_M]$. Since it is a 2π-periodic function we model it as a Fourier polynomial $P_0(\alpha)$ of order m:

$$P_0(\alpha) = \frac{a_0 + a_m}{2} + \sum_{k=1}^{m} a_k \cos(k\alpha) + b_k \sin(k\alpha), \quad (2)$$

$$\text{where } a_k = \frac{2}{M} \sum_{i=1}^{M} P(\alpha_i) \cdot \cos(k\alpha_i) \quad (3)$$

$$\text{and } b_k = \frac{2}{M} \sum_{i=1}^{M} P(\alpha_i) \cdot \sin(k\alpha_i). \quad (4)$$

The function $P_0(\alpha)$ fits exactly the experimental data at the measured points $\boldsymbol{\alpha}$ if $m = M/2$. However, a fairly small value of m (i.e., $m \ll M/2$) is already a good approximation to the measurements, as can be seen in Fig. 2(b).

C. Beacon network setup

Assume N Bluetooth low energy beacons placed at different positions in an environment. The i-th beacon is placed at position $\boldsymbol{S}_i = [s_{x,i}, s_{y,i}]^T$, while the position of the user (smartphone) at a certain point in time is given by $\boldsymbol{U}_j = [u_{x,j}, u_{y,j}]^T$. Thus it holds for the distance between the i-th beacon and the j-th smartphone's position $d_{ij} = \sqrt{(s_{x,i} - u_{x,j})^2 + (s_{y,i} - u_{y,j})^2}$, and the angle α_{ij} from the beacon towards the smartphone is given by $\alpha_{ij} = \arctan((s_{y,i} - u_{y,j})/(s_{x,i} - u_{x,j}))$.

III. Cramér-Rao lower bound

According to the log-normal fading model of Eq. (1), the measurement noise is normally distributed: $n \sim \mathcal{N}(0, \sigma_n^2)$. With the beacon positions assumed to be known, the probability density function (PDF) of the received signal strength at user position $\boldsymbol{U}_j$ is given by

$$p_{P|\boldsymbol{U}}(P_{i,j}|\boldsymbol{U}_j) = \frac{1}{\sqrt{2\pi}\sigma_n} \exp\left(\frac{-1}{2\sigma_n^2}\left(P_{i,j} - \overline{P}_{i,j}\right)^2\right) \quad (5)$$

with

$$\overline{P}_{i,j} = P_0(\alpha_{i,j}) - 10\eta \ln(d_{i,j}) \quad (6)$$

$$= \frac{a_0 + a_m}{2} + \sum_{k=1}^{m} a_k \cos(k\,\alpha_{i,j}) + b_k \sin(k\,\alpha_{i,j}) - 5\eta \ln\left((s_{x,i} - u_{x,j})^2 + (s_{y,i} - u_{y,j})^2\right) \quad (7)$$

where we have set the reference distance to $d_0 = 1$ [m]. Here, $\overline{P}_{i,j}$ is the expected mean RSSI value of the i-th beacon at position $\boldsymbol{U}_j$. Assuming that we have N i.i.d. observations we get for the log likelihood

$$l_{\boldsymbol{U}_j} = -\sum_{i=1}^{N} \ln\left\{\sqrt{2\pi}\sigma_n\right\} - \frac{1}{2{\sigma_n}^2} \sum_{i=1}^{N} \left(P_{i,j} - \overline{P}_{i,j}\right)^2. \quad (8)$$

For the Cramér-Rao lower bound we calculate the derivatives of (8) with respect to $u_{x,j}$ and $u_{y,j}$ up to the second order. For the first oder derivative we get

$$\frac{\partial l_{\boldsymbol{U}_j}}{\partial u_{x,j}} = \frac{1}{\sigma_n^2} \sum_{i=1}^{N} \left(P_{i,j} - \overline{P}_{i,j}\right) \cdot \frac{\partial}{\partial u_{x,j}} \left(\overline{P}_{i,j}\right) \quad (9)$$

and for the second order, respectively

$$\frac{\partial^2 l_{\boldsymbol{U}_j}}{\partial u_{x,j}\partial u_{x,j}} = -\frac{1}{\sigma_n^2}\sum_{i=1}^{N}\frac{\partial}{\partial u_{x,j}}\left(\overline{P}_{i,j}\right)\cdot\frac{\partial}{\partial u_{x,j}}\left(\overline{P}_{i,j}\right) + \frac{1}{\sigma_n^2}\sum_{i=1}^{N}\left(P_{i,j}-\overline{P}_{i,j}\right)\cdot\frac{\partial^2}{\partial u_{x,j}\partial u_{x,j}}\left(\overline{P}_{i,j}\right) \quad (10)$$

The second order derivatives with respect to $u_{x,j}$ and $u_{y,j}$ are

$$\frac{\partial^2 l_{\boldsymbol{U}_j}}{\partial u_{x,j}\partial u_{y,j}} = -\frac{1}{\sigma_n^2}\sum_{i=1}^{N}\frac{\partial}{\partial u_{x,j}}\left(\overline{P}_{i,j}\right)\cdot\frac{\partial}{\partial u_{y,j}}\left(\overline{P}_{i,j}\right) + \frac{1}{\sigma_n^2}\sum_{i=1}^{N}\left(P_{i,j}-\overline{P}_{i,j}\right)\cdot\frac{\partial^2}{\partial u_{x,j}\partial u_{y,j}}\left(\overline{P}_{i,j}\right). \quad (11)$$

The Cramér-Rao lower bound on the variance of the k-th dimension of the position estimate $\hat{\boldsymbol{U}}_j$ is then given by

$$var(\hat{\boldsymbol{U}}_{j,k}) \geq (J^{-1}(\boldsymbol{U}_j))_{kk} \quad (12)$$

with

$$J(\boldsymbol{U}_j) = -E\left\{\begin{bmatrix}\frac{\partial^2}{\partial u_{x,j}\partial u_{x,j}}l_{\boldsymbol{U}_j} & \frac{\partial^2}{\partial u_{x,j}\partial u_{y,j}}l_{\boldsymbol{U}_j}\\ \frac{\partial^2}{\partial u_{y,j}\partial u_{x,j}}l_{\boldsymbol{U}_j} & \frac{\partial^2}{\partial u_{y,j}\partial u_{y,j}}l_{\boldsymbol{U}_j}\end{bmatrix}\right\}. \quad (13)$$

The square root of the sum of the diagonal elements $(J^{-1}(\boldsymbol{U}_j))_{kk}$ is a lower bound for the root mean squared error (RMSE) of the position estimate $\hat{\boldsymbol{U}}_j$:

$$RMSE(\hat{\boldsymbol{U}}_j) \geq \sqrt{tr\left\{J^{-1}(\boldsymbol{U}_j)\right\}} \quad (14)$$

All derivatives are summarized in a box at the end of the paper.

Please note the following: The derivation of the CRLB utilizes the derivative of the likelihood at the ground truth value of the parameter to be estimated, and the expectation of the derivative w.r.t. the measurements has to be taken. Thus the expected values of the second order derivatives can be simplified, since $E[P_{i,j}-\overline{P}_{i,j}]=0$. In case of eq. (10) we obtain

$$E\left[\frac{\partial^2 l_{\boldsymbol{U}_j}}{\partial u_{x,j}\partial u_{x,j}}\right] = -\frac{1}{\sigma_n^2}\sum_{i=1}^{N}\left(\frac{\partial}{\partial u_{x,j}}\overline{P}_{i,j}\right)^2, \quad (15)$$

since the expected value of the second part of eq. (10) equals zero.

IV. Simulation Results

Positioning using beacons with known directivity pattern can be expected to have a lower CRLB than positioning with omnidirectional radiation patterns, because the known directivity adds position dependent information. This is indeed the case as can be seen by the simulation results of Fig. 3.

In Fig. 3 a setup with three beacons in a room of size $3.5\ m \times 5\ m$ is depicted. The left plot shows the undirected model with a typical region of increased RMS error on the interconnection line between the two upper beacons and a significant error in front of the third beacon. The right plot shows more dark blue colors than the left plot, which means that the average RMSE inside the room is reduced by the introduction of directed beacon models. The black whisker at the beacons indicates the direction of maximum radiation.

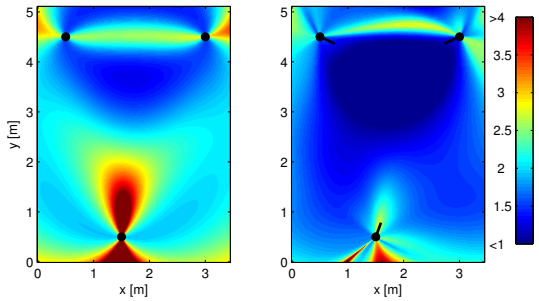

Fig. 3. Root CRLB, see eq. (14), in [m]: Comparison between model with omnidirectional characteristic (see eq. (1)), left figure; and angular dependent model with parameters from lab measurements (see eq. (2)), right figure.

Instead of straight lines of increased errors between beacons we now find curved regions of increased error. Also isolated error "hotspots" in the vicinity of the beacons with a sharp increase of the error compared to adjacent regions can be observed. Note, that the RMSE and the position of the error hotspots mainly depend on the direction of the beacons.

A. Experiments with randomized beacon directions

In order to get an impression of the dependence of the localization error on each beacon's orientation in a BLE network, we present experiments with randomly generated setups.

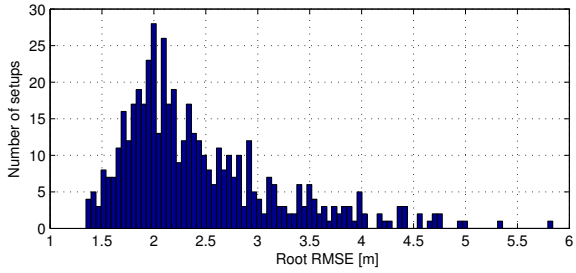

Fig. 4. Histogram of average root CRLB values for experiments with a fixed beacon geometry using different, randomly selected beacon directions for each experiment.

For the results in Fig. 4 we kept the positions of the three beacons fixed and drew the orientation of each beacon uniformly at random. For each configuration we calculated the root CRLB averaged over 150 positions placed on a regular grid in the room of size given above. The Fig. 4 displays the histogram of the average root CRLBs of 500 configurations. The best setup achieves an RMSE of less than 1.5 m while the worst ones exceed an RMSE of 4 m (see Fig. 5). These results clearly show the potential benefits of integrating direction information into the beacon network planning process.

By having a close look at the results we could formulate the following guidelines for the choice of beacon orientation

- Avoiding symmetries in the setups improves results. Simply pointing all beacons into the center of the room

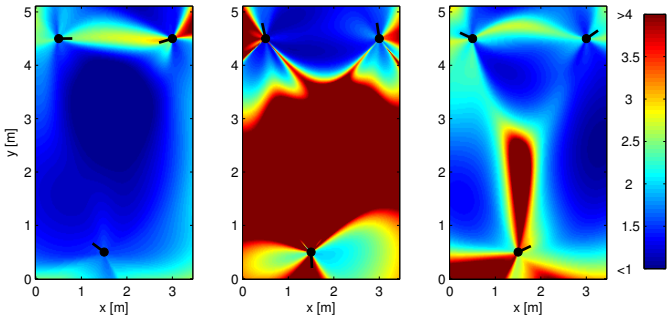

Fig. 5. Best, worst and an average result from randomly generated beacon directions in terms of root CRLB in [m]

will create symmetry effects and regions within the room with an increased error

- Pointing the beacon's power maximum towards the region of interest in a space is beneficial for the overall error.

We should mention that we could verify these effects also in real setups.

B. Localization experiments

A straightforward ML estimator of the user location works as follows: For each grid point we evaluate eq. (5) using the observed beacon RSSI values and the expected signal strength at the grid point following eq. (7). The grid point with the highest likelihood is chosen as the smartphone's position.

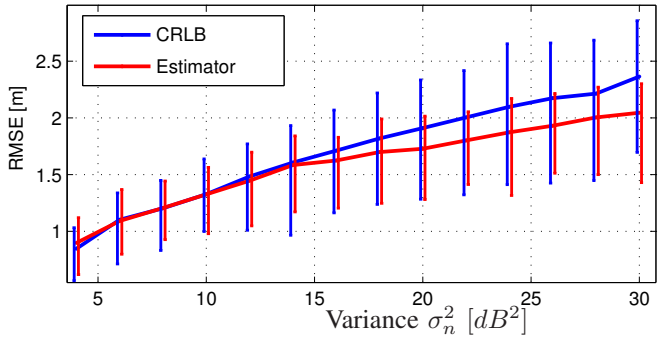

Fig. 6. Comparison between root CRLB and RMSE of grid approach estimator.

We generated random geometries consisting of four beacons in a room of size $7\,\mathrm{m} \times 10\,\mathrm{m}$, and calculated the ML position estimate from simulated observations. The results are compared with the root CRLB in Fig. 6 for different values of the variance σ_n^2 of the log-normal fading. For each variance value the figure shows the mean value and the Min-Max spread found in 150 random geometries.

The position estimator reaches the CRLB for small variances and even exceeds it for larger variance values. This unexpected result could be traced back to the fact that the ML estimator is bound to select a point within the room limiting the error by the size of the room, whereas the CRLB is ignorant w.r.t. the room boundaries.

V. Sensor placement optimization

Placing beacons in a room with the intention to minimize the localization error at any given position is a problem which is similar to planing the network coverage of wireless communication systems, which is known to be NP-hard [14].

In order to find a solution with manageable computational effort we implemented the following suboptimal approach, which is based on an evolutionary optimization algorithm [15], see Fig. 7. First an initial set of P randomly generated geometries is created. For each geometry the average CRLB for a grid of points is calculated as a cost function to evaluate the geometry. The B geometries with the smallest costs are kept and directly forwarded to the next generation set. The remaining geometries are recombined and mutated to form additional $(P - B)$ geometries, see explanation below. Together with the B best ones they form the new generation of geometries, which is again evaluated with respect to the CRLB.

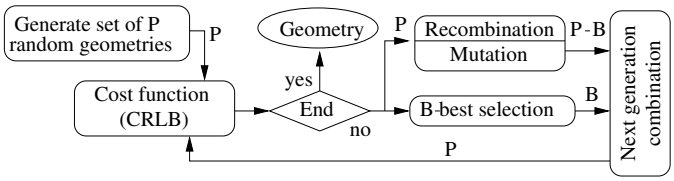

Fig. 7. Evolutionary optimization algorithm

The recombination procedure randomly selects two geometries, where the likelihood to be drawn is inversely proportional to the cost function ("survival of the fittest"). From the selected geometries we randomly select beacons, subsequently add random values to their positions and orientation values (mutation step) and put them into the new geometry until the amount of desired beacons per room is reached. The random selection of beacons is proportional to the minimum distance to beacons in the new geometry, i.e. drawing a beacon which is close to the position of an already selected beacon is unlikely. Distance based drawing improves the overall area coverage and reduces the amount of iterations.

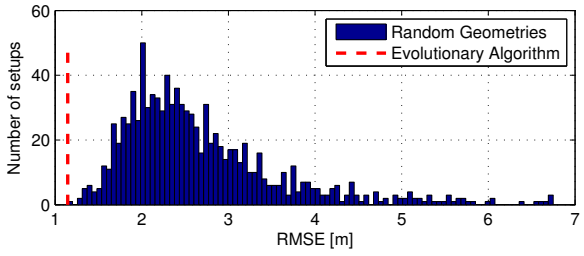

Fig. 8. Histogram of average root CRLB values of 1000 randomly generated geometries, and the result of the evolutionary algorithm

In Fig. 8 the histogram of average root CRLB values obtained from 1000 randomly generated geometries of a 3-beacon network and a room size of $3.5\,\mathrm{m} \times 5\,\mathrm{m}$) are depicted. The red dashed line shows the result of the evolutionary algorithm after 10 iterations with a population size of $P = 20$.

VI. Conclusions

In this paper we have used Fourier polynomials to describe angular dependent radio patterns of Bluetooth low energy beacons. The Cramér-Rao lower bound for position estimation was derived, assuming a log-normal fading model. This result was then used to calculate the localization errors to be expected for a given BLE network geometry. Additionally, an evolutionary algorithm for finding a near-optimal beacon placement was presented.

$$\frac{\partial}{\partial u_{x,j}}\overline{P}_{i,j} = \frac{10\eta\left(s_{x,i}-u_{x,j}\right)}{{d_{ij}}^2} - \frac{\left\{\sum_{k=1}^{m} a_k k\sin\left(k\alpha_{ij}\right) - b_k k\cos\left(k\alpha_{ij}\right)\right\}\left(s_{y,i}-u_{y,j}\right)}{{d_{ij}}^2} \tag{16}$$

$$\begin{aligned}\frac{\partial^2\overline{P}_{i,j}}{\partial u_{x,j}\partial u_{x,j}} &= \frac{10\eta}{{d_{ij}}^2} - \frac{20\eta\left(s_{x,i}-u_{x,j}\right)^2}{{d_{ij}}^4} + \frac{\left\{\sum_{k=1}^{m} a_k k^2\cos\left(k\alpha_{ij}\right) + b_k k^2\sin\left(k\alpha_{ij}\right)\right\}\left(s_{y,i}-u_{y,j}\right)^2}{{d_{ij}}^4} \\ &+ \frac{2\left\{\sum_{k=1}^{m} a_k k\sin\left(k\alpha_{ij}\right) + b_k k\cos\left(k\alpha_{ij}\right)\right\}\left(s_{y,i}-u_{y,j}\right)^3}{{d_{ij}}^4\left(s_{x,i}-u_{x,j}\right)} - \frac{2\left\{\sum_{k=1}^{m} a_k k\sin\left(k\alpha_{ij}\right) - b_k k\cos\left(k\alpha_{ij}\right)\right\}\left(s_{y,i}-u_{y,j}\right)}{{d_{ij}}^2\left(s_{x,i}-u_{x,j}\right)}\end{aligned} \tag{17}$$

$$\frac{\partial}{\partial u_{y,j}}\overline{P}_{i,j} = \frac{10\eta\left(s_{y,i}-u_{y,j}\right)}{{d_{ij}}^2} + \frac{\left\{\sum_{k=1}^{m} a_k k\sin\left(k\alpha_{ij}\right) - b_k k\cos\left(k\alpha_{ij}\right)\right\}\left(s_{x,i}-u_{x,j}\right)}{{d_{ij}}^2} \tag{18}$$

$$\frac{\partial^2\overline{P}_{i,j}}{\partial u_{y,j}\partial u_{y,j}} = \frac{10\eta}{{d_{ij}}^2} - \frac{20\eta\left(s_{y,i}-u_{y,j}\right)^2}{{d_{ij}}^4} + \frac{\left\{\sum_{k=1}^{m} a_k k^2\cos\left(k\alpha_{ij}\right) + b_k k^2\sin\left(k\alpha_{ij}\right)\right\}}{\left(s_{x,i}-u_{x,j}\right)^{-2}{d_{ij}}^4} - \frac{2\left\{\sum_{k=1}^{m} a_k k\sin\left(k\alpha_{ij}\right) - b_k k\cos\left(k\alpha_{ij}\right)\right\}}{\left\{\left(s_{y,i}-u_{y,j}\right)\left(s_{x,i}-u_{x,j}\right)\right\}^{-1}{d_{ij}}^4} \tag{19}$$

$$\begin{aligned}\frac{\partial^2\overline{P}_{i,j}}{\partial u_{y,j}\partial u_{x,j}} &= \frac{\partial^2\overline{P}_{i,j}}{\partial u_{x,j}\partial u_{y,j}} = \frac{20\eta\left(s_{x,i}-u_{x,j}\right)\left(s_{y,i}-u_{y,j}\right)}{{d_{ij}}^4} + \frac{\left\{\sum_{k=1}^{m} a_k k^2\cos\left(k\alpha_{ij}\right) + b_k k^2\sin\left(k\alpha_{ij}\right)\right\}\left(s_{x,i}-u_{x,j}\right)\left(s_{y,i}-u_{y,j}\right)}{{d_{ij}}^4} \\ &+ \frac{2\left\{\sum_{k=1}^{m} -a_k k\sin\left(k\alpha_{ij}\right) + b_k k\cos\left(k\alpha_{ij}\right)\right\}\left(s_{y,i}-u_{y,j}\right)^2}{{d_{ij}}^4} + \frac{\left\{\sum_{k=1}^{m} a_k k\sin\left(k\alpha_{ij}\right) - b_k k\cos\left(k\alpha_{ij}\right)\right\}}{{d_{ij}}^2}\end{aligned} \tag{20}$$

References

[1] D. Gorecky, M. Schmitt, M. Loskyll, and D. Zuhlke, "Human-machine-interaction in the industry 4.0 era," *12th IEEE International Conference on Industrial Informatics (INDIN 2014)*, pp. 289–294, 2014.

[2] A. Asthana, M. Cvavatts, and P. Krzyzanowski, "An Indoor Wireless Systeim for Personalized Shopping Assistance," in *Workshop on Mobile Computing Systems and Applications, 1994.*, 1994, pp. 69–74.

[3] R. Ban, K. Kaji, K. Hiroi, and N. Kawaguchi, "Indoor Positioning Method Integrating Pedestrian Dead Reckoning with Magnetic Field and WiFi Fingerprints," *Eight International Conference on Mobile Computing and Ubiquitous Networking (ICMU 2015)*, pp. 167–172, 2015.

[4] M. K. Hoang, J. Schmalenstroeer, and R. Haeb-umbach, "Aligning Training Models with Smartphone Properties in WIFI Fingerprinting based Indoor Localization," in *IEEE International Conference on Acoustic, Speech and Signal Processing (ICASSP 2015)*, 2015, pp. 1981–1985.

[5] M. K. Hoang, J. Schmalenstroeer, C. Drueke, D. H. T. Vu, and R. Haeb-Umbach, "A hidden Markov model for indoor user tracking based on WiFi fingerprinting and step detection," *Proceedings of the 21st European Signal Processing Conference (EUSIPCO), 2013*, pp. 1–5, 2013.

[6] S. Lee, B. Koo, M. Jin, C. Park, M. J. Lee, and S. Kim, "Range-free indoor positioning system using smartphone with bluetooth capability," *IEEE/ION Position, Location and Navigation Symposium - PLANS 2014*, pp. 657–662, 2014.

[7] H. Liu, H. Darabi, P. Banerjee, and J. Liu, "Survey of Wireless Indoor Positioning Techniques and Systems," *IEEE Transactions on Systems, Man, and Cybernetics, Part C: Applications and Reviews*, vol. 37, no. 6, pp. 1067–1080, 2007.

[8] S. He and S.-H. G. Chan, "Wi-Fi Fingerprint-based Indoor Positioning: Recent Advances and Comparisons," *IEEE Communications Surveys and Tutorials*, 2015.

[9] R. Faragher and R. Harle, "Location Fingerprinting with Bluetooth Low Energy Beacons," *IEEE Journal on Selected Areas in Communications*, vol. 33, no. 11, 2015.

[10] M. Altini, D. Brunelli, E. Farella, and L. Benini, "Bluetooth indoor localization with multiple neural networks," *IEEE 5th International Symposium on Wireless Pervasive Computing 2010*, pp. 295–300, 2010.

[11] N. Patwari, A. Hero, M. Perkins, N. Correal, and R. O'Dea, "Relative location estimation in wireless sensor networks," *IEEE Transactions on Signal Processing*, vol. 51, no. 8, pp. 2137–2148, Aug 2003.

[12] M. Hossain and W. S. Soh, "Cramér-Rao bound analysis of localization using signal strength difference as location fingerprint," in *Proceedings - IEEE INFOCOM*, no. 1, 2010.

[13] A. D. Angelis and C. Fischione, "Mobile Node Localization via Pareto Optimization : Algorithm and Fundamental Performance Limitations," *IEEE Journal on Selected Areas in Communications*, vol. 33, no. 7, pp. 1288–1303, 2015.

[14] A. Krause, A. Singh, and C. Guestrin, "Near-Optimal Sensor Placements in Gaussian Processes-Theory, Efficient Algorithms and Empirical Studies," *The Journal of Machine Learning Research*, vol. 9, no. May, pp. 235–284, 2008.

[15] T. Bäck, *Evolutionary Algorithms in Theory and Practice: Evolution Strategies, Evolutionary Programming, Genetic Algorithms*. Oxford University Press, 1996.